The Minimization of Torque Ripples of Segmental Type Switched Reluctance Motor by Particle Swarm Optimization

H. Terzioğlu*[1], S. Herdem[2], G. Bal[3]

Abstract: In this study, we realized a controller design which can reduce torque ripple of 10/8 Switched Reluctance Motor (SRM). To perform the study, a Switched Reluctance Motor with 5 phase, U type segmental rotor was used. The control of the SRM was actualized by bipolar converter used H-bridge topology. The control signals of converter are obtained by control circuit designed by using dsPIC33EP512MU810. One of the reasons of the current ripples in the SRM is ON-OFF times in a period of the control signals. When the ripples of the current reduced, the ripples of torque of the SRM also reduced. Therefore, in this study, the ON-OFF times in a period of phase control signals were determined by an algorithm used particle swarm optimization. When SRM was controlled by this algorithm developed, the decreasing of its torque ripples was determined.

Keywords: Segmental Type Switched Reluctance Motor, H-Bridge Converter, dsPIC33, Torque Ripple, PSO

1. Introduction

Switched Reluctance Motors (SRM) are the electrical machines which have been used widely in recent years. They have a simple and enduring structure, low-cost, low inertia, high speed, high efficiency and a high performance [1]. Whereas the place of the use of SRMs is increasing, their torque ripples and the acoustic noise are the most important disadvantages for them [2]. In most of the works performed so far, this problem has been tried to be solved through the physical structure of the motor, drive circuit or control circuit. In the works that were carried out, a new 5-phase and U shape SRM with a segmental rotor was designed and it was stated that this new designed SRM produced more torque than the classical SRM [3, 4].

Many studies have been performed to reduce the torque ripple that is the most important problem of SRMs. The ripples in the torque were minimized by using a method called Torque Sharing Function (TSF). In this method, the reference torque value was directly turned into reference analytical wave by analytical method. It is a study performed using this method and arranging triggering angles. Linear and sinusoidal TSF method was used and compared, and the torque ripples were minimized [5]. In the control of 8/6 SRM, the starting and ending angles of the triggering angles of power switches were determined and a new approach was brought [6]. For SRM a direct torque control was recommended with Lyapunov function stability based. The magnetic properties of SRM have an indirect structure (because torque, phase current and rotor positions have complicated positions). Torque ripples were minimized through the method

recommended in this study [7]. The effects of the stator pole shape over moment ripples were searched in SRMs. As a result of the studies, a motor design with a high average moment production and with low moment ripples was fulfilled [8]. It is stated that the converter structure that is used in the control of SRM affects the overall performance of the system and the loss of the motor and torque ripples are the factors to be taken into account while evaluating the motor [9]. Besides, another study was also carried out to determine proportion between rotor and stator thread width inside SRM for a high torque and proper output power [10]. By using B-spline neural network (BSNN), torque ripples of the SRM were reduced. Closed loop torque control was performed using an online torque estimator. Because of local weight updating algorithm used for BSNN, a proper phase current profile was obtained as real-time so as to reduce torque ripples and it was expressed that it had a good dynamic performance according to the changes in the desired torque. It was explained that the suggested schema did not require a current controller with high bandwidth and the validity of the schema was shown by simulations and experimental results [11]. Speed regulation was carried out by using Adjustable Fuzzy Cerebellar Model Articulation Controller [12]. ANN model was used to determine the rotor position of SRM. Three methods were compared to each other: Traditional ANN, Developed ANN and the method where developed ANN and curve fitting were used together [13]. Sudden torque control was performed by using linear magnetic model. Torque control was performed by determining commutation angle. It was seen in the results of the simulation and experiment that torque ripple decreased [14]. The speed of SRM was checked by using the method of Takagi-Sugeno-Kang (TSK) Fuzzy Controller [15]. A new stable technique was developed for the speed control applications of Switched Reluctance Motor and the mathematical model of SRM was used in this technique. In this study, Second Order Sliding Mode Control (SOSMC) and a super twisting algorithm schema were used [16]. The speed control of on grid Switched Reluctance Generator that was driven by wind turbine was checked by using Adaptive ANN controller [17]. A 5- phase segmental type SRM was designed to increase the torque in SRMs. Also, a bipolar driving strategy was used to increase the

---

[1] *Electrical and Electronic Engineering, Institute of Science and Technology of Selcuk University*
[2] *Department of Electrical and Electronics Engineering, Engineering Faculty, Selcuk University.*
[3] *Department of Electrical and Electronics Engineering, Faculty of Technology, Gazi University.*
* Corresponding Author: Email: hterzioglu@selcuk.edu.tr*

torque even more. A traditional full bridge converter was used. A higher torque output was obtained as a result of bipolar driving method [18]. A new SRM was designed by placing auxiliary winding and permanent magnet in the stator yoke of Switched Reluctance Motor. The traditional SRM and newly designed SRM were tested by asymmetrical half-bridge [19]. 50 kW- SRM was designed for hybrid electrical vehicles (Toyota Prius 2003). Designed SRM and stable magnetic synchronous motor were compared. It was seen that the performance of the newly designed SRM was 95% and it reached the targeted torque at the rate of 85% [20]. The vibration and the noise of the motor could be reduced by the changes in the design and control system of the motor and it was also stated that triggering angles affected the torque ripple of the motor [21].

In this study, optimum triggering angle values were determined so as to reduce the torque ripples of the 5 –phase 10/8 segmental type SRM (ST-SRM). Particle Swarm Optimization (PSO) was used to determine optimum triggering angles. Triggering angle values which were determined by PSO were applied to H-bridge driving circuit by SnadPIC PIC Microchip Development Board with dsPIC33EP512MU810 on it and ST-SRM was checked as a bipolar. As a result of the experimental study, the effects of triggering style of SRM motor on motor torque was also determined.

2. Segmental Type Switched Reluctance Motor

In this study, 10/8 segmental type SRM (ST-SRM) that has a different rotor type from a classical SRM was used. The rotor of the ST-SRM motor consists of both the parcels formed by laminated silicon steel and an aluminium block in which these parcels are placed. The aluminium block that is used in rotor structure functions as a flux barrier and this speciality isolates the motor from classical SRMs. It can be called as U shape segmental type motor because the rotor type of segmental type SRM is U shape. The sectional view of Segmental Type Switched Reluctance Motor is seen in Figure 1 [22].
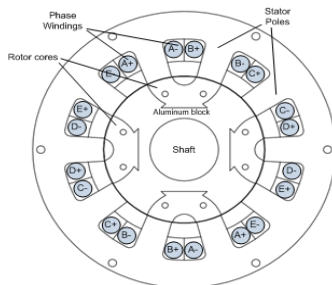

Figure 1. The view of 5-phase segmental type SRM

The features of Segmental Type Switched Reluctance Motor are given at Table 1.

Table 1. The features of Segmental Type Switched Reluctance Motor

No	Features	Value
1	Maximum moment at 5 A	2.34 Nm
2	Maximum inductance	13 mH
3	Stator phase resistance	0.86 Ω
6	Magnetic field energy at 5 A	0.848 Joule
7	Moment/weight ratio	0.22 Nm/kg
8	Phase number	5
9	Stator/Rotor Configuration	10/8
14	Stator phase angle	0.314 rad
15	Rotor phase angle	0.331 rad

3. Indirect Mathematical Model of Segmental Type Switched Reluctance Motor

When magnetic hysteresis loss, Eddy current loss and phase winding are omitted, the mathematical expressions of SRM are given in Equation (1) [23].

$$V_k = R_k\,i_k + \left(L_k + i_k\,\frac{\partial L_k}{\partial \theta}\right)\frac{di_k}{dt} + i_k\,\frac{\partial L_k}{\partial \theta}\,\frac{d\theta}{dt} \tag{1}$$

When phase winding mutual inductance is omitted in Equation (1), θ refers to rotor position, i_k refers to current, L_k refers to winding inductance for each phase, R_k refers to phase winding resistance.

The rotor position of the motor can be converted to angular speed as in Equation (2).

$$\omega = \frac{d\theta}{dt} \tag{2}$$

In this case, when the expression in Equation (1) is written in its place in Equation (2), it is also described as in Equation (3) that is mathematical model of equivalent circuit of SRM.

$$V_k = R_k\,i_k + \left(L_k + i_k\,\frac{\partial L_k}{\partial \theta}\right)\frac{di_k}{dt} + \omega\,i_k\,\frac{\partial L_k}{\partial \theta} \tag{3}$$

In Equation (3), it is seen that the source voltage equals the total of 3 voltages. To show k phase circuit, the first voltage is the voltage drop in the resistance; the second voltage is the transformer electromotive force caused by the changed flux because the current was changed; the third one is about electromechanical energy of SRM caused by the changed flux because the position of the rotor was changed [24].

Torque statement of one phase of SRM is given in Equation (4).

$$T_{e_k} = \frac{1}{2}i_k^{\,2}\,\frac{dL_k\left(\theta, i_k\right)}{d\theta} \tag{4}$$

In SRMs, m is the phase number and total electrical torque produced in the motor can be calculated as in Equation (5).

$$T_e = \sum_{k=1}^{m} T_{e_k} \tag{5}$$

Mechanical modelling of SRM can be calculated as in Equation (6).

$$T = T_e - T_y = J\,\frac{d\omega}{dt} + B\omega \tag{6}$$

In Equation (6), ω is angular speed, T_L is load torque, B is friction coefficient and J is inertia.

Torque ripple of SRM is calculated as in Equation (7).

$$\%T_{ripple} = \frac{T_{max} - T_{min}}{T_{avg}}.100 \tag{7}$$

4. Accuracy of the Modelling

Accuracy is a value that shows how close the calculated value is the measured value. Equation (8) is used for every data value to determine the error value between the value measured and the value that is calculated or estimated.

$$\delta_i = \frac{\left|R_a - R_a^{\,0}\right|}{R_a}*100 \tag{8}$$

Here δ_i is the error of each data, R_a is estimated results, $R_a^{\,0}$ is experimental results and i is data index.

Equation (9) is used to determine total errors of whole model.

$$\Delta = \frac{1}{n}\sum_{i}^{n}\delta_i \tag{9}$$

Here Δ is the estimated accuracy of the model, n is number of data.

Error ratio of the torque ripple was determined by using Equation (8) and (9).

International Journal of Intelligent Systems and Applications in Engineering

5. Particle Swarm Optimization

PSO is a heuristic algorithm that was developed by James Kennedy and Russell Eberhart in 1995 [25]. This is a heuristic algorithm that exists in all living creatures in the nature and based on social intelligence. Human beings share the knowledge by talking, the birds make use of each other to find their directions and a school of fish decides their behavior through a mutual decision and all these attitudes are the evidence of a social being. PSO was developed being inspired of the birds' making use of each other for directions and the mutual behaviors of the fish [26]. PSO shows similarities with evolutionary optimization techniques like GA but it does not have evolutionary operators (crossbreeding and mutation). The solutions called as particles in PSO travel in the problem space by following the best results within the solutions.

PSOs are easier to carry out when compared to GA and the number of the parameters to be arranged is lower. For this reason, PSOs are used in many fields today as an application. [26]. Flow chart of PSO is seen in Figure 2.
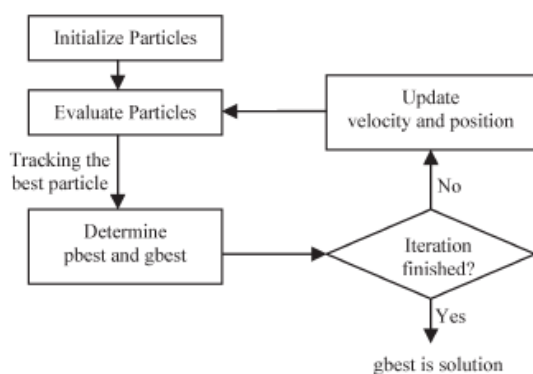

Figure 2. PSO flow chart

General steps of PSO algorithm can be listed as follows [27];
1. Population is created. Initial value and the speed of each particle are casually assigned.
2. Suitability value of each particle is calculated according to the objective function.
3. The best value of the particle is found. The suitability value found out in the previous step is compared to the best personal value (pbest) that is in the memory of the particle. If the result found out in the previous step is better than the current ''pbest'' value, the new value is changed as ''pbest.''
4. The best global particle is found. The suitability value that is calculated for each particle in the second step is compared to the best global value ''gbest'' that is kept in the memory of the program. If there is a better result, this result is changed with ''gbest.''
5. The speed and speed factor of the particle are arranged according to Equation (10) and the position of the particle is arranged according to Equation (11). r_1 ve r_2 are the numbers produced between [0,1].

$$v_i^{k+1} = w\,v_i^k + c_1 r_1 (pbest_i^k - x_i^k) + c_2 r_2 (gbest^k - x_i^k) \qquad (10)$$

$$x_i^{k+1} = x_i^k + v_i^{k+1} \qquad (11)$$

6. The processes between the steps of 2-5 are repeated until the ending condition or conditions are fulfilled.

6. Test Functions

To determine the accuracy of the PSO algorithm software, algorithm was worked on the functions that were known before and their performances were evaluated. For this reason, PSO algorithm was tried by using some functions that were known in the literature and the accuracy of the unit software was determined. A test function group that consists of the Benchmark functions seen in the Table 2 was created so as to inspect the accuracy of the unit software prepared in MATLAB. The mathematical expressions in the test functions at Table 2 were tried in PSO [28-30]. The particle number in PSO whose unit software was performed was approached as 100 and learning coefficient was approached as 2. Ending criteria was accepted as 1000 for iteration number or 0 for error value.

Table 2. Test Functions

	Function name	Funciton	Limits
F1	Sphere	$F_1 = \sum_{i=1}^{4} x_i^2$	$[-150, 75]$
F2	Rosenbrock	$F_2 = \sum_{i=1}^{4} \left[100\left(x_{i+1} - x_i^2\right)^2 + \left(x_i - 1\right)^2 \right]$	$[-50, 25]$
F3	Rastrigin	$F_3 = \sum_{i=1}^{4} \left[10 + x_i^2 - 10\cos(2\pi x_i) \right]$	$[-50, 25]$

Instead of working PSO algorithm once and getting a result from it, the average of the results that are received after working it many times are accepted. For this reason, PSO algorithm was worked 20 times and the averages were accepted as results, then they were given in Table 3. For the test functions, global minimum solutions that were carried out in the previous studies were given in Table 4.

Table 3. Solutions of the Test Functions

Algorithm Functions	Global Minimum Values	PSO Solutions
F1	0	2.65E-8
F2	0	6E-4
F3	0	14.8E-2

7. Material and Method

In this study, the reduction of the ripple values in the torque was aimed to reduce by arranging the ON and OFF time of the signal when the phase windings are energized. Here, the PSO algorithm determines signals to be used angularly. As seen in Figure 3, it was thought that one triggering signal was applied to one phase. 3 different position values seen in the figure were optimized. This means that the number of the factors in the algorithm is 3. The number of the factors was determined as 3 because increasing this number would make it difficult for the current to reach the desired value. Phase limit in the Figure 3 was determined as the ending position of the each phase. The limits of the factors in the PSO algorithm were determined as 4≤θ₁≤8, 8≤θ₂≤13, 13≤θ₃≤17 by taking into account the increasing and decreasing times of the current.
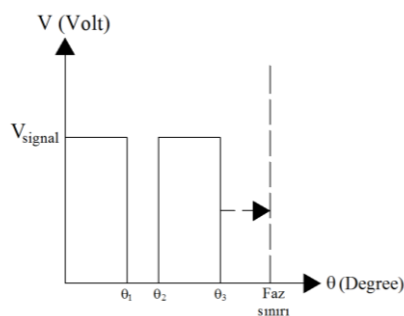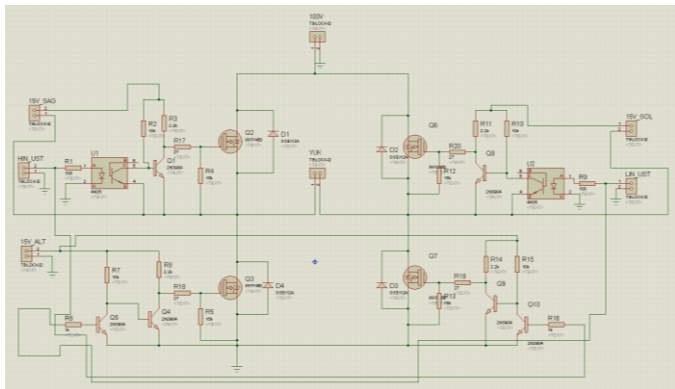

Figure 3. Phase triggering signal

Optimum angle values that are produced when PSO algorithm is worked are given in Table 4.

Table 4. PSO algorithm result and torque ripple

PSO			
θ_1	θ_2	θ_3	T_{ripple}
7.2^0	11^0	16.4^0	%33.4

8. Experiment Setup and the Results

In this study, H-Bridge converter structure, with the control of dsPIC33EP512MU810, was used for the segmental type SRM.
A phase circuit of the H-Bridge that was designed in Proteus program is given in Fig. 4.

Figure 4. A driving circuit and H-Bridge of a phase

In this study, the motor was run as bipolar. The sequence of trigger signals of 5 phase segmental type SRM is given in Table 5 [3]. In the performed studies, the sequence of the triggering was performed as in Table 5.

Table 5. Triggering Sequence of the Phases

|	0-18	18-36	36-54	54-72	72-90
A Phase	0	+	0	-	0
B Phase	-	0	0	+	0
C Phase	+	0	-	0	0
D Phase	0	0	+	0	-
E Phase	0	-	0	0	+

The experiments were performed using the testing apparatus set up in Fig 5.

Figure 5. The picture of the testing apparatus

In this study RD300 model of FUTEK brand, with 0-10 Nm measuring range, was used to measure motor torque. The signal received from the torque sensor was increased to 0-5 V voltage level using FUTEK brand CSG110 amplifier. The motor speed was measured by 3600 pulse Autonics brand encoder. Motor current was measured using ACS712 current sensor. The signals received from current and torque sensors and the encoder were transferred to the computer, to the interface designed at Visual C# by SnadPIC PIC Microchip Development Board. In the designed interface, torque and current interface were both displayed in the screen and saved in the data base.

7.2^0, 11^0, 16.4^0 triggering angles that were determined by PSO algorithm and the torque ripple of the ST-SRM that was controlled as bipolar were calculated as 31.9 % as seen in the interface screen in Figure 6.
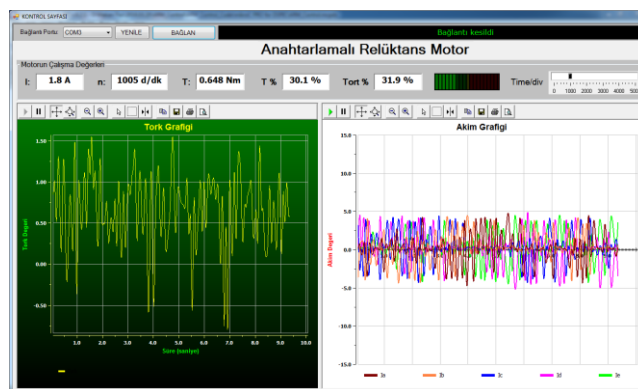
Figure 6. The results of the SRM triggered at 7.2, 11, 16.4 degree.

Torque ripple values of PSO obtained as a result of the algorithm and the torque ripple values obtained experimentally are seen at Table 6.

Table 6. PSO algorithm and experimental results

	Torque Ripple
T_{ripple} (PSO)	33.4
T_{ripple} (Experimental)	31.9
Error Value (%)	5.83

As seen at Table 6, there is a 5.83 % error value between the torque ripple values obtained by PSO algorithm and obtained experimentally. This value shows that PSO gave a successful performance for a system with a quite difficult modeling. Besides, in the previous studies performed on ST-SRM which was used in this study, the motor had a 56 % torque ripple [3, 4]. For this reason, the control signal of the motor was changed in this study and a 40.35% reduction was obtained in the torque ripple.

9. Conclusions

In this study, the controlling of the 5–phase 10/8 Segmental Type SRM was carried out by H-bridge converter topology that was controlled by dsPIC33EP512MU810. The angle values of the triggering signal recommended for the control of ST-SRM were determined by means of PSO algorithm. When compared to the previous studies, there was a 40.35% reduction in the torque ripple of the ST-SRM that worked with the values obtained from PSO algorithm. This shows that heuristic algorithm could produce a successful result about torque ripple that is the most important disadvantage of the SRMs. In the next studies, by using different heuristic algorithm or changing the parameter values of the PSO, their effects on the torque ripple of the motor can be searched.

REFERENCES

[1] Terzioglu H., Bal G., and Herdem S., "The Modelling of Variation Inductance For Segmental Type Switched Reluctance Motors," presented at the 7th International Advanced Technologies Symposium (IATS'13), Istanbul, Turkey, 2013.

[2] G. Bal, *Özel elektrik makinaları*: Seçkin Yayıncılık, 2011.

[3] Uygun D., "5-Fazlı U-Tipi Segmental Rotorlu Bipolar Uyartımlı 10/8 Anahtarlamalı Relüktans Motorun Tasarımı Ve Uygulaması," Ph.D.. Thesis, Fen Bilimleri Enstitüsü Elektrik Eğitimi, Gazi Üniversitesi, 2012.

[4] D. Uygun, G. Bal, and I. Sefa, "Linear Model of a Novel 5-Phase Segment Type Switched Reluctance Motor," *Elektronika ir Elektrotechnika*, vol. 20, pp. 3-7, 2014.

[5] V. P. Vujičić, "Minimization of torque ripple and copper losses in switched reluctance drive," *IEEE transactions on power electronics*, vol. 27, pp. 388-399, 2012.

[6] S. AbouHashesh, M. El-Nemr, and E. Rashad, "Correlative angles switching technique for switched reluctance motor drive systems," in *GCC Conference and Exhibition (GCCCE), 2015 IEEE 8th*, 2015, pp. 1-6.

[7] S. K. Sahoo, S. Dasgupta, S. K. Panda, and J.-X. Xu, "A Lyapunov function-based robust direct torque controller for a switched reluctance motor drive system," *IEEE Transactions on Power Electronics*, vol. 27, pp. 555-564, 2012.

[8] Y. K. Choi and C. S. Koh, "Pole Shape Optimization of Switched Reluctance Motor for Reduction of Torque Ripple," in *2006 12th Biennial IEEE Conference on Electromagnetic Field Computation*, 2006.

[9] M. Liptak, "Principle of Design of Four-phase Low-power Switched Reluctance Machine Aimed: to the Maximum Torque Production," *Journal of Electrıical Engineering-Bratislava*, vol. 55, pp. 138-143, 2004.

[10] B. G., D. Uygun, "An approach to obtain an advisable ratio between stator and rotor tooth widths in switched reluctance motors for higher torque and smoother output power profile," *Gazi University Journal of Science*, vol. 23, pp. 457-463, 2010.

[11] Z. Lin, D. S. Reay, B. W. Williams, and X. He, "Torque Ripple Reduction in Switched Reluctance Motor Drives Using B-Spline Neural Networks," *IEEE Transactions on Industry Applications*, vol. 42, pp. 1445-1453, 2006.

[12] S.-Y. Wang, C.-L. Tseng, and S.-C. Chien, "Adaptive fuzzy cerebellar model articulation control for switched reluctance motor drive," *IET electric power applications*, vol. 6, pp. 190-202, 2012.

[13] R. Zhong, Y. Wang, and Y. Xu, "Position sensorless control of switched reluctance motors based on improved neural network," *IET Electric Power Applications*, vol. 6, pp. 111-121, 2012.

[14] C. Moron, A. Garcia, E. Tremps, and J. Somolinos, "Torque control of switched reluctance motors," *IEEE Transactions on Magnetics*, vol. 48, pp. 1661-1664, 2012.

[15] C.-L. Tseng, S.-Y. Wang, S.-C. Chien, and C.-Y. Chang, "Development of a self-tuning TSK-fuzzy speed control strategy for switched reluctance motor," *IEEE Transactions on Power Electronics*, vol. 27, pp. 2141-2152, 2012.

[16] M. Rafiq, S.-u. Rehman, F.-u. Rehman, Q. R. Butt, and I. Awan, "A second order sliding mode control design of a switched reluctance motor using super twisting algorithm," *Simulation Modelling Practice and Theory*, vol. 25, pp. 106-117, 2012.

[17] H. M. Hasanien and S. Muyeen, "Speed control of grid-connected switched reluctance generator driven by variable speed wind turbine using adaptive neural network controller," *Electric Power Systems Research*, vol. 84, pp. 206-213, 2012.

[18] R. Vandana, S. Nikam, and B. Fernandes, "High torque polyphase segmented switched reluctance motor with novel excitation strategy," *IET electric power applications*, vol. 6, pp. 375-384, 2012.

[19] Y. Hasegawa, K. Nakamura, and O. Ichinokura, "A novel switched reluctance motor with the auxiliary windings and permanent magnets," *IEEE Transactions on Magnetics*, vol. 48, pp. 3855-3858, 2012.

[20] M. Takeno, A. Chiba, N. Hoshi, S. Ogasawara, M. Takemoto, and M. A. Rahman, "Test results and torque improvement of the 50-kW switched reluctance motor designed for hybrid electric vehicles," *IEEE Transactions on Industry Applications*, vol. 48, pp. 1327-1334, 2012.

[21] E. O. a. H. K. M. Polat, "Control of Switched Reluctance Motor and Examination of Effect on the Torque Ripple of the Trigger Points," presented at the 6th International Advanced Symposium (IATS'11), Elazıg, Turkey, 2011.

[22] D. Uygun, "Design and Application Of 5-Phase Bipolar Excited 10/8 Switched Reluctance Motor With U-Type Segmental Rotor Pairs," PhD thesis, Electrical Education, Gazi University, Graduate School of Natural and Applied Sciences, 2012.

[23] N. J. Nagel and R. D. Lorenz, "Modeling of a saturated switched reluctance motor using an operating point analysis and the unsaturated torque equation," *IEEE transactions on industry applications*, vol. 36, pp. 714-722, 2000.

[24] Y.-L. Cui, X.-C. Yu, H.-L. Fan, and J.-B. Fan, "The simulation study for switched reluctance motor drives based on Matlab 6.5," in *2005 International Conference on Machine Learning and Cybernetics*, 2005, pp. 1076-1081.

[25] İ. Akbulut, "Parçacık Sürü Optimizasyonu ile Anten Tasarımı " Yüksek Lisans, Mühendislikte İleri Teknolojiler, İstanbul Teknik Üniversitesi, Bilişim Enstitüsü, 2009.

[26] H. Eldem, "Karınca Koloni Optimizasyonu (KKO) ve Parçacık Sürü Optimizasyonu (PSO) Algortimaları Temelli Bir Hiyerarşik Yaklaşım Geliştirilmesi " Yüksek Lisans, Bilgisayar Mühendisliği, Selçuk Üniversitesi, Fen Bilimleri Enstitüsü, 2014.

[27] H. Demirci, "Parçacık Sürü Optimizasyonu ve Çoğalan Sürü Algoritmasının Yüzey Geri Çatımı Problemşnde Uygulanması ve Karşılaştırılması," Yüksek Lisans, Bilgisayar ve Bilişim Mühendisliği, Sakarya Üniversitesi, Fen Bilimleri Enstitüsü, 2011.

[28] M. Y. Özsağlam and M. Cunkaş, "Optimizasyon Problemlerinin Çözümü için Parçaçık Sürü Optimizasyonu Algoritması," *Politeknik Dergisi*, vol. 11, 2008.

[29] Erdoğmuş P. and E. Yalcin, "Parçacık Sürü Optimizasyonu ile Kısıtsız Optimizasyon Test Probleminin Çözümü " *İleri Teknoloji Bilimleri Dergisi*, vol. 4, 2015.

[30] S. Kiranyaz, T. Ince, and M. Gabbouj, *Multidimensional particle swarm optimization for machine learning and pattern recognition*: Springer, 2014.